Available online at www.sciencedirect.com
SCIENCE DIRECT®
Engineering Structures 26 (2004) 1333–1347
ENGINEERING STRUCTURES
www.elsevier.com/locate/engstruct

# Experimental evaluation of extended endplate beam-to-column joints subjected to bending and axial force

L.R.O. de Lima [a], L. Simões da Silva [b,*], P.C.G. da S. Vellasco [a], S.A.L. de Andrade [a,c]

[a] Structural Engineering Department, UERJ—State University of Rio de Janeiro, Rio de Janeiro, Brazil
[b] Civil Engineering Department, University of Coimbra, Polo II, Pinhal de Marrocos, Coimbra 3030-290, Portugal
[c] Civil Engineering Department, PUC-RIO—Pontifical Catholic University of Rio de Janeiro, Rio de Janeiro, Brazil

Received 2 February 2004; accepted 13 April 2004

**Abstract**

Steel beam-to-column joints are often subjected to a combination of bending moment and axial force. Current specifications for steel joints do not take into account the presence of axial forces (tension and/or compression) in the joints. A single empirical limitation of 5% of the beam's plastic axial capacity is the only enforced provision in Eurocode 3—Part 1.8. The objective of the present paper is to describe an experimental program carried out at the University of Coimbra on extended endplate beam-to-column joints to try to extend the component method philosophy to the combined action of bending moment and axial force. To fulfil this objective, a set of seven extended beam-to-column joints were tested. This paper provides a detailed description of this experimental programme focusing on the moment–rotation curves and individual component assessment. Finally, it reveals that the presence of an axial force on the beam significantly modifies the joint response.


*Keywords:* Component method; Experimental analysis; Extended endplate joints; Semi-rigid behaviour; Bending moment and axial force

## 1. Introduction

### 1.1. Generalities

Commonly, beam-to-column joints and beam splices are subjected to a combination of bending moment and axial force. A typical example of such situation is illustrated in Fig. 1.

Joints subjected to combination of bending moment ($M$) and axial force ($N$) usually operate around two typical situations:

(i) low values of the $M/N$ ratio, characteristic of column base joints. In this case, all bolt rows are usually not active (in compression) and the neutral axis often lies inside the section.
(ii) high values of the $M/N$ ratio, characteristic of beam-to-column joints. In this case, it is common that during a specific loading history, there is reversal of bolt row forces.

Currently, no specific provisions are available for the analysis and design of beam-to-column joints under bending and axial forces in the context of part 1.8 of Eurocode 3 [1]. Historically, for the high $M/N$ ratio range, the revised version of Annex J [2] proposed a single empirical limitation on the allowable axial force of 10% of the beam axial plastic resistance, below which the axial force could be disregarded in the analysis.

For column bases (low $M/N$ ratio), specific procedures where developed during the late 1990s [3–5], that are now incorporated into part 1.8 of EC3 [1]. Despite the differences between column bases and beam-to-column joints, the former already cover some aspects relevant to the latter case. In particular, they identify the different situations corresponding to the various possible positions of the neutral axis. However, column bases miss all aspects related to the contribution of the column web panel to the beam-to-column joint response.

Adopting the component method as the framework, this lack of guidance motivated a coordinated effort within the ECCS, Technical Committee 10, "Connec-

* Corresponding author. Tel.: +351-239-797-216; fax: +351-239-797-217.
*E-mail address:* luisss@dec.uc.pt (L. Simões da Silva).

0141-0296/$ - see front matter © 2004 Elsevier Ltd. All rights reserved.
doi:10.1016/j.engstruct.2004.04.003

**Nomenclature**

| | |
|---|---|
| $K$ | individual component stiffness |
| $E$ | Young's modulus |
| $F_{Rd}$ | individual component resistance |
| $F_{Rd\ row}$ | row component resistance |
| $M_{j,Rd}$ | bending moment capacity |
| $S_{j,ini}$ | joint initial stiffness |
| $\sigma_1$ and $\sigma_2$ | principal stresses |
| $\sigma_{VM}$ | *von Mises* stress |

tions'' (TWG 10.2), to develop explicit rules. This paper briefly reviews the current developments and describes in detail the experimental work performed on extended endplate beam-to-column joints carried out at the University of Coimbra, Portugal.

### 1.2. Experimental background

A summary of the experimental work on beam-to-column joints under combined bending moment and axial force is presented below. Guisse et al. [6] performed tests on six prototypes of column bases with extended endplates with bolts placed outside of the beam height and six more tests on flush endplates with bolts inside the beam height. Although related to column bases, these tests provided some relevant information. The experimental test layout and the configuration of the joints are presented in Fig. 2. Two different endplate thicknesses (15 and 30 mm) were used and three levels of axial force, i.e., 100, 400 and 1000 kN for first series and 100, 600 and 1000 kN for second series. The compressive axial force was applied first and kept constant during the test while the bending moment was subsequently increased up to failure.

Wald and coauthors [4] performed two tests at the Technical University in Prague on beam-to-beam and beam-to-column joints. The loading application system used in these tests may be observed in Fig. 3(a) and led to proportional increase of axial force and bending

Fig. 1. Example of a pitched-roof portal frame joint.

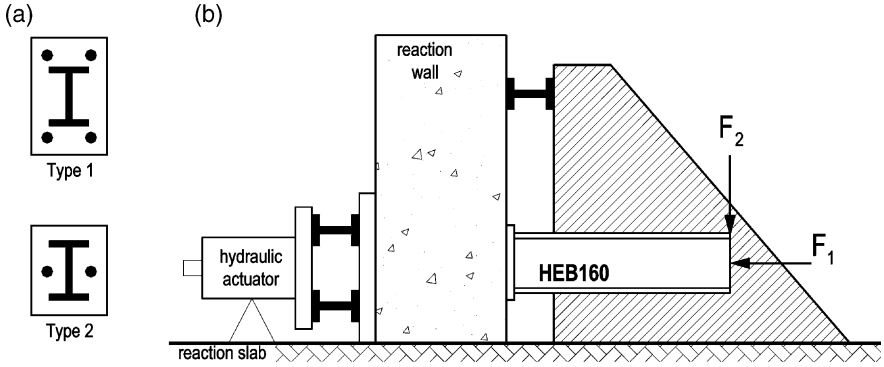


Fig. 2. Guisse et al.'s test information [6]. (a) Joint type and (b) experimental test layout.

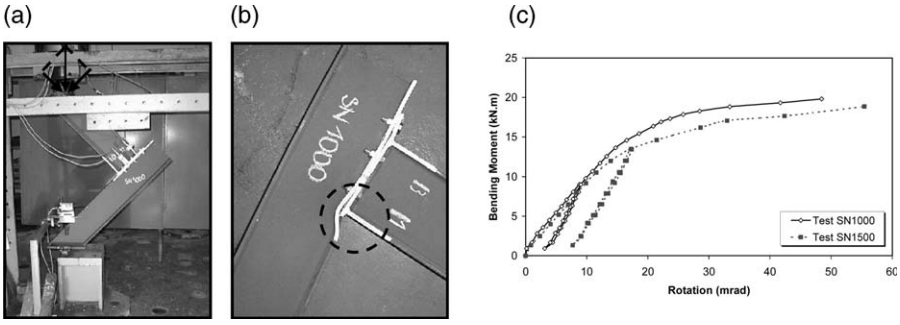


Fig. 3. Test layout and moment versus rotation curves for tests performed by Wald and coauthors [4]. (a) Test layout, (b) joint residual deformation and (c) beam-to-column moment versus rotation curves.

moment. The resulting deformed configurations and moment versus rotation curves are presented in Fig. 3(b) and (c), respectively. From these two tests, it could be concluded that the bending moment resistance in test SN1000 was greater than that in the second test, in line with the different level of applied axial force. For both tests, failure occurred at the column flange in the compression zone. Unfortunately, no test with only bending moment was performed, which prevented the determination of the influence of the axial force in the joint response.

An experimental programme using endplate beam-to-column joints was performed at the Civil Engineering Department of the University of Coimbra, Portugal. The test programme included 15 prototypes, i.e., eight flush endplate joints and seven extended endplate joints. The results of the flush endplate tests may be found in Refs. [8–10] while the extended endplate tests will be discussed in detail in this paper. The adopted loading strategy for the flush endplate joints consisted of an initial application of the total axial force (tension or compression), kept constant during the test and the subsequent incremental application of the bending moment. These tests have shown that the presence of axial force may significantly affect the joint response in terms of bending resistance. For low levels of compressive axial force, an increase of the bending resistance was observed. On the other hand, the presence of tensile axial force on the joint caused immediate reduction of the bending resistance due to premature yielding of the critical joint component in the tension zone, i.e., endplate in bending. Fig. 4 shows the deformed joints for tests FE6 (compressive axial force of 27% of the beam plastic resistance) and FE9 (tensile axial force of 20% of the beam plastic resistance), respectively.

### 1.3. Analytical models

Recently, several analytical models have been proposed in order to predict the behaviour of beam-to-column joints under bending and axial force. At the University of Liège, Jaspart [11,12], Finet [13] and Cerfontaine [14] have applied the principles of the component method to develop design predictions of the $M$–$N$ interaction curves and initial stiffness.

The investigation performed in Liège proposed that the beam-to-column joint subjected to bending and

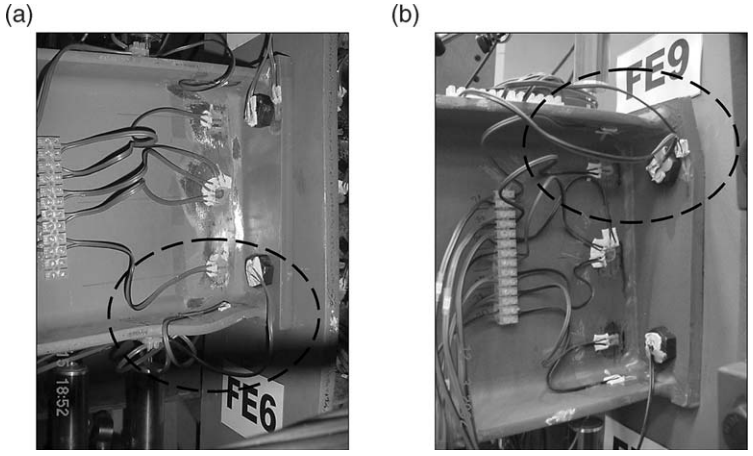


Fig. 4. Failure of flush endplate beam-to-column joints [10]. (a) Test FE6 ($N = -27\%\ N_{pl}$)—beam flange in compression and (b) test FE9 ($N = +20\%\ N_{pl}$)—endplate in bending.

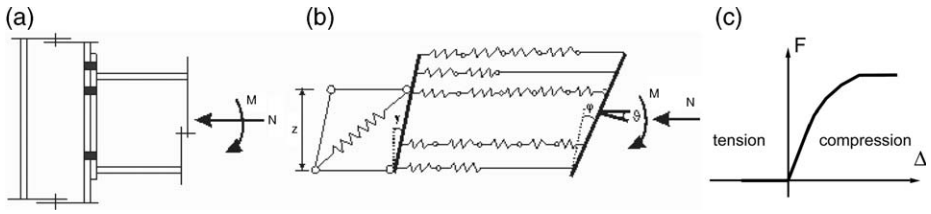


Fig. 5. Mechanical model developed in Liège [14]. (a) Beam-to-column joint, (b) mechanical model and (c) component behaviour.

compressive axial force may be characterized with the aid of Fig. 5, where the response of each compressive component is simulated by an extensional spring whose behaviour may be observed in Fig. 5(c).

Based on the same general principles, Silva and Coelho [15] have proposed analytical expressions for the full non-linear response of a welded beam-to-column joint under combined bending and axial force. In this model, each non-linear spring was replaced with two equivalent elastic springs using an energy formulation and a post-limit stability analysis. This analytical model was applied to a welded joint extracted from SERICON II database [16], but the comparison with test results was performed without considering the presence of the axial force.

Sokol et al. [17] proposed an analytical model to predict the behaviour of joints subjected to bending moment and axial force for proportional loading, i.e., the axial force and the bending moment are simultaneously increased. This model was calibrated through comparison with experimental tests performed by Wald and Švarc [7].

Table 1 presents a summary of recent studies performed to investigate the joints behaviour subjected to bending moment and axial force.

## 2. Experimental programme

### 2.1. General description

The experimental program on extended endplate beam-to-column joints consisted of seven tests comprising several combinations of bending moment and axial force. In all tests, the joint configuration was identical (Fig. 6), the column being simply supported at both ends and consisting of an HEB240, the beams sections were IPE240 and the endplate was 15 mm thick, all manufactured from a steel S275. The bolts were M20, grade 10.9, pre-stressed with a torque of 150 Nm.

The seven tests were performed by first applying a fixed level of axial tension or compression and subsequently imposing a negative bending moment, incremented up to the joint failure. In the first test, EE1, only bending moment was applied. For the following tests, EE2, EE3, EE4, EE5, EE6 and EE7, constant axial forces of, respectively, −10%, −20%, −27%, −15%, +10% and + 20% of the beam plastic resistance were applied to the beam.

### 2.2. Test setup, instrumentation and testing procedure

The test setup is illustrated in Fig. 7(a) with the bending moment being applied through a hydraulic actuator, located 1 m away from the column flange face.

The adopted compressive axial force application system consisted of a central hydraulic jack located behind the reaction wall, Fig. 7(b), that applies a tensile force to four pre-stressing cables with diameter $\phi = 15.2$ mm. The transfer of this force to the connection was performed through a 600 kN central load cell, Fig. 7(c). These cables pass through a deviator saddle (HEM100) to guarantee that the axial force is always parallel to the beam axis and 200 kN load cells were

Table 1
Summary of studies of joints subjected to bending and axial force

| Authors (date) | Analysis type | Country and Institution |
|---|---|---|
| Finet (1994) [13] | Analytical model | University of Liège (Belgium) |
| Jaspart (1997) [11] | Analytical model and experimental tests | |
| Cerfontaine (2001) [14] | Analytical model | |
| Silva and Coelho (2001) [15] | Analytical model | University of Coimbra (Portugal) |
| Simões da Silva et al. (2001) [8] | Analytical model | |
| Lima (2003) [10] | Experimental tests | |
| Wald and Švarc (2001) [7] | Experimental tests | Prague University (Czech Republic) |
| Sokol et al. (2002) [17] | Analytical model | |

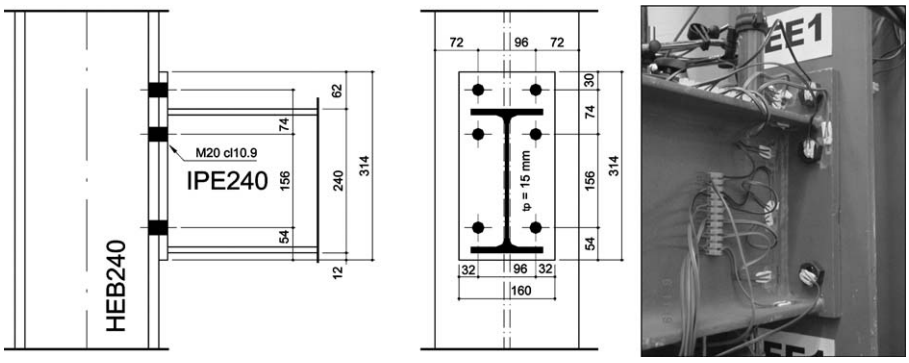


Fig. 6. Extended endplate beam-to-column joint layout.

used in each cable to monitor the installed cable forces, Fig. 8. The horizontal reaction forces at both ends of the column were transmitted to the reaction wall by: (i) a steel beam, at the top, and (ii) a reinforced concrete footing pre-stressed to the strong floor using DYWIDAG bars and connected to the reaction wall using an HEB200, at the bottom.

The tensile axial force application system is shown in Fig. 9(a). Four hydraulic jacks located in one of the extremities of a circular hollow section profile transmit the tensile axial force. These circular profiles are simply supported in the other end to allow free rotation and to guarantee that the axial force is always applied parallel to the beam axis. The hydraulic jacks are connected to the same hydraulic system in order to apply equal amounts of load to the four cables, Fig. 9(b).

All tests were instrumented as depicted in Fig. 10, with linear strain gauges (FLK 6-11-TML), rosettes at 45° (FRA 5-11-TML), bolt axial strain gauges (BTM 6-C-TML), and displacements transducers (LVDTs). All data were recorded with a data acquisition system TDS602-TML.

For all tests, a constant axial force was applied first, maintained constant throughout the test, with the subsequent application of a bending moment incremented up to failure. Two unloading phases were performed. The first, for a bending moment of 100 kN m (down to 20 kN m, to eliminate possible slack in the joint) and the second for a rotation of 50 mrad. Force control was used in the first part of each test, subsequently changed to displacement control in the latter part.

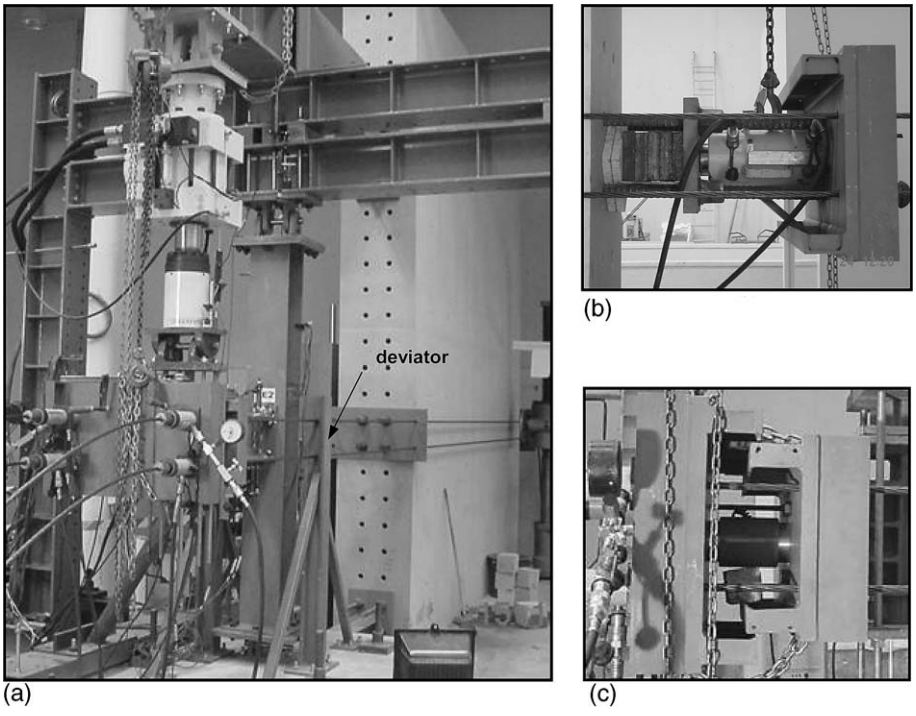


Fig. 7. (a) Compressive axial loading frame, (b) hydraulic jack and (c) central load cell.

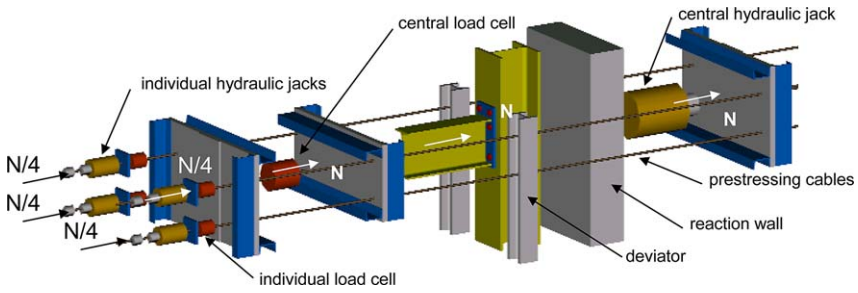


Fig. 8. Compressive axial load application system.

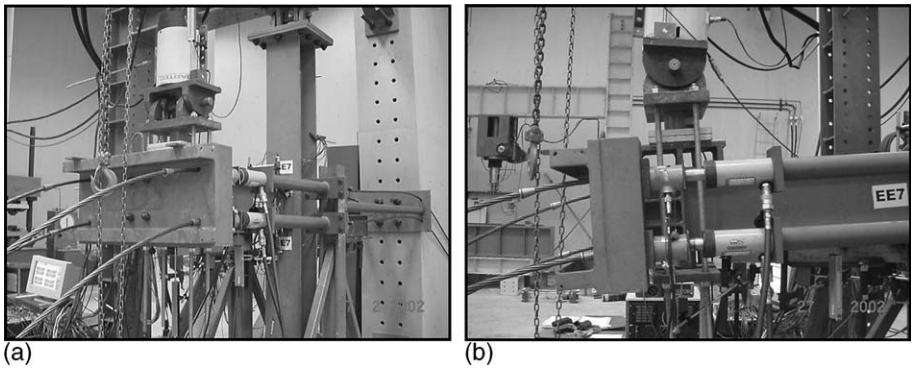


Fig. 9. (a) Tensile axial application system and (b) hydraulic jack layout.

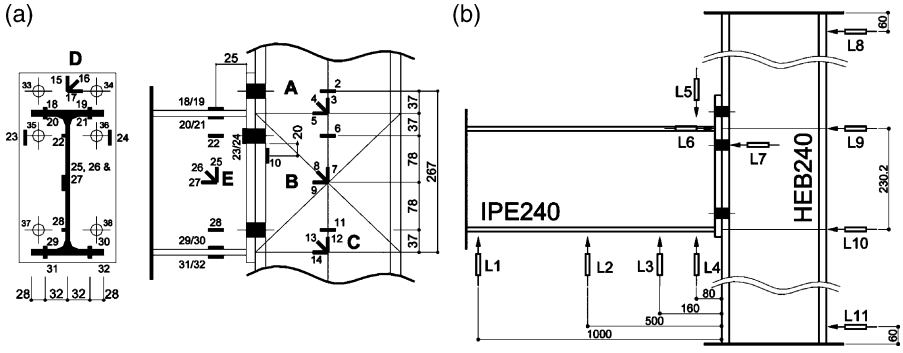


Fig. 10. Instrumentation layout. (a) Linear strain gauges, rosettes and bolt axial strain gauges layout and (b) displacement transducers layout.

## 3. Experimental results

### 3.1. Material properties

Tensile tests on coupons extracted from the beams and columns were carried out, aiming to characterize the actual material properties. With these results in hand, it was possible to calculate the beam plastic resistance and to determine the actual level of applied axial force to the beam during the tests. These tensile tests were performed according to the following specifications, EN10002 [18], EN10020 [19] and EN10025 [20], yielding the results of Table 2.

### 3.2. Moment–rotation curves

The moment–rotation curves for all tests are illustrated in Fig. 11, where it can be observed that the presence of the axial force in joints influences the joint behaviour.

The maximum bending moment resistance was obtained for test EE2, whose compressive axial force level corresponded to 10% of the beam plastic resistance, leading to a value 6% greater than test EE1 without axial loads. For all other levels of compressive axial force, the maximum bending moments were smaller than test EE2. For the two tests with tensile axial force, EE6 and EE7, the bending moment resistance

Table 2
Steel mechanical properties

| Specimen | | $f_y$ (MPa) | $f_u$ (MPa) | Young's modulus (MPa) |
|---|---|---|---|---|
| *Beam IPE240* | | | | |
| Web | Average | 363.4 | 454.3 | 203 713 |
| | SD | 17.64 | 7.49 | 7214 |
| Flange | Average | 340.14 | 448.23 | 215 222 |
| | SD | 18.08 | 7.38 | 3017 |
| *Column HEB240* | | | | |
| Web | Average | 372.02 | 477.29 | 206 936 |
| | SD | 28.56 | 19.59 | 8206 |
| Flange | Average | 342.95 | 448.79 | 220 792 |
| | SD | 5.68 | 27.39 | 9516 |
| *Endplate* | | | | |
| Endplate | Average | 369.44 | 503.45 | 200 248 |
| | SD | 10.62 | 8.05 | 1694 |

was less than the EE1 test due to premature mobilization of the components in the joint tension zone. Table 3 summarizes these results.

### 3.3. Analysis of the individual components

The breakdown of the extended endplate joint into its individual components is best visualized in Fig. 12, that illustrates the relevant components and the corresponding component model for the pure bending case. The corresponding components are (1) column web panel in shear, (2) column web in compression, (3) column web in tension, (4) column flange in bending, (5) endplate in bending, (7) beam flange and web in compression, (8) beam web in tension, and (10) bolts in tension.

An application of the Eurocode 3 procedure for bending moment alone leads to the results of Table 4 (using actual material properties and dimensions and no partial safety coefficients). It is noted that only the two top bolt rows were considered in tension following the recommendations presented in Eurocode 3, Part 1.8 that disregard the contribution of any bolt row that is close to the centre of compression, i.e., the component's lever arm is smaller than 40% of its distance from the farthest bolt row.

From Table 4 results, it is clear that the joint compression zone controls the behaviour while the critical component was associated to the beam flange in compression.

Starting with the column web panel in shear, large deformations are expected for this component, since the joint corresponds to an external column. Examination of Fig. 13(a), that presents the principal stresses measured with aid of the rosette "B", located in the centre of the column web panel in shear, shows that this component reached the yielding limit in all tests.

Analysing the results of *von Mises* stresses obtained at the same point, Fig. 13(b), it was observed that for the first test, EE1, the yielding limit was reached for a bending moment equal to 98 kN m, being the lowest bending level where this component reached the yielding limit. On the other hand, the highest resistance was verified in the second test, EE2, at 121 kN m, associated to the test that presented the greater bending resistance.

The column web in compression is characterized in Fig. 14, with the strains being measured with the aid of channels 11 and 14. Channel 14 represents the strain deformations in the centre of the compressive region, greater than the values measured by channel 11. Once again, the presence of the axial force modifies the global response of this component. It is observed that this component did not reach yield in any of the tests, in line with the analytical results in Table 4.

The beam flange in compression was evaluated using the four strain gauges located in the beam compression flange, Fig. 10. This component is critical and, as expected, the yielding limit was reached in all tests. Fig. 15(a)

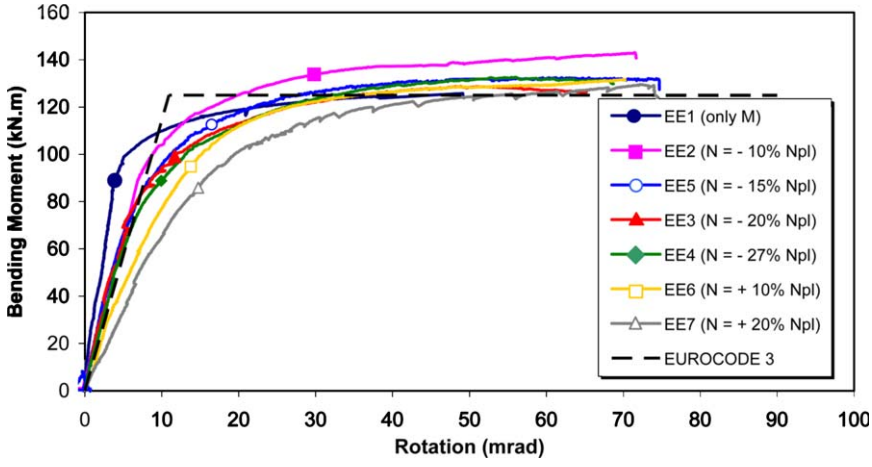


Fig. 11. Experimental tests: moment versus rotation curves.

Table 3
Experimental bending moments ($M_{j,Rd}$) and initial stiffness ($S_{j,ini}$)

| Test | $N$ (kN) | $M_{j,Rd}$ (kN m) | $M_{j,Rd}/M_{j,Rd\ EE1}$ | $S_{j,ini}$ (kN m/rad) |
|---|---|---|---|---|
| EE1 (only $M$) | – | 118.7 | 1.00 | 20 290 |
| EE2 ($-10\%\ N_{pl}$) | −135.94 | 125.4 | 1.06 | 15 685 |
| EE3 ($-20\%\ N_{pl}$) | −193.3 | 118.1 | 0.99 | 16 228 |
| EE4 ($-27\%\ N_{pl}$) | −259.2 | 113.2 | 0.95 | 16 668 |
| EE5 ($-15\%\ N_{pl}$) | −363.5 | 111.9 | 0.94 | 17 046 |
| EE6 ($+10\%\ N_{pl}$) | 127.2 | 111.5 | 0.94 | 13 060 |
| EE7 ($+20\%\ N_{pl}$) | 257.9 | 101.0 | 0.85 | 14 905 |

presents the average of the measured strains: it is clear that in the tests with compressive axial force, the yielding limit was reached for lower levels of bending moment than in the tensile axial force tests. Fig. 15(b) depicts the residual deformations of test EE3, clearly identifying the beam flange local buckling.

Strain gauge 10 and LVDT 7 were used to assess the component column flange in bending. Fig. 16 shows that this component only reached the yielding limit in test EE7. This was caused by the high level of tensile axial force (corresponding to 20% of the beam plastic resistance). Additionally, for all tests with compressive axial forces, this component remained in compression.

Fig. 17 illustrates the moment–strain curves for the endplate in bending, obtained with two linear strain gauges corresponding to channels 23 and 24, respectively. This component controls the behaviour of the joint in the tensile zone. For the tests with compressive axial force, an increase of the component resistance is observed, in contrast to the tests with tensile force.

The curves depicted in Fig. 18 associated to the principal stresses obtained through rosette "D" indicate that the deformations in the top region of the endplate correspond to bending in the horizontal axis, confirming the assumption of Eurocode 3, Part 1.8 [1] of a vertical "T-stub" used to simulate this component. Fig. 19 illustrates the *von Mises* stresses evaluated with the same rosette, the yielding limit being reached in all tests.

Finally, the bolts in tension were analysed using the data from the bolt strain gauges. Fig. 20(a) shows the moment versus strain results for all bolts of test EE1, where it can be observed that the bottom bolt row

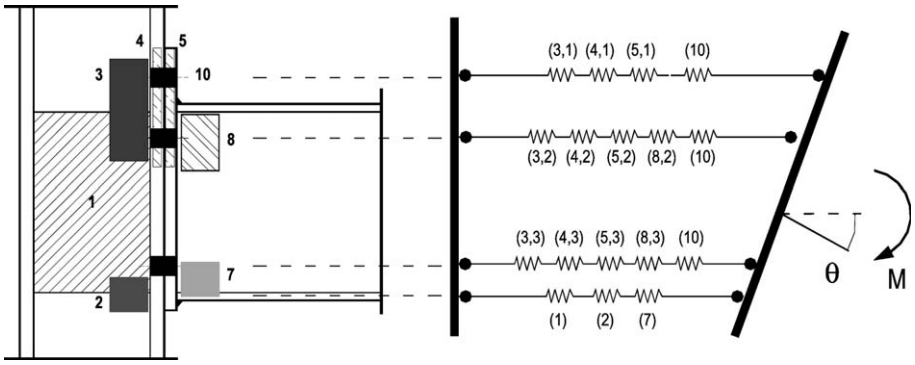


Fig. 12. Component identification and corresponding component model for bending.

Table 4
Component evaluation according to Eurocode 3

| | Component | $F_{Rd}$ (kN) | $k/E$ (mm) | $F_{Rd\ row}$ (kN) |
|---|---|---|---|---|
| First bolt row in tension ($h = 267.1$ mm) | Column web in tension (3) | 533.2 | 5.74 | 274.5 |
| | Column flange in bending (4) | 408.3 | 31.21 | |
| | Endplate in bending (5) | 274.5 | 19.00 | |
| | Bolts in tension (10) | 441.0 | 7.76 | |
| Second bolt row in tension ($h = 193.1$ mm) | Column web in tension (3) | 460.6 | 4.91 | 267.7 |
| | Column flange in bending (4) | 408.3 | 26.7 | |
| | Endplate in bending (5) | 332.4 | 13.35 | |
| | Beam web in tension (8) | 483.0 | $\infty$ | |
| | Bolts in tension (10) | 441.0 | 7.76 | |
| Compression | Column web in shear (1) | 642.5 | 5.68 | 542.2 |
| | Column web in compression (2) | 654.3 | 10.4 | |
| | Beam flange in compression (7) | 542.2 | $\infty$ | |

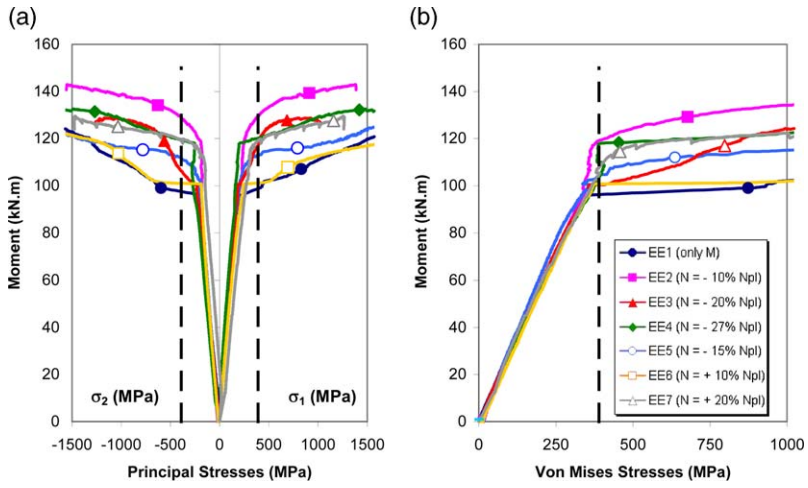


Fig. 13. Column web in shear (1)—moment *versus* stress curves. (a) $\sigma_1$ and $\sigma_2$, and (b) $\sigma_{VM}$.

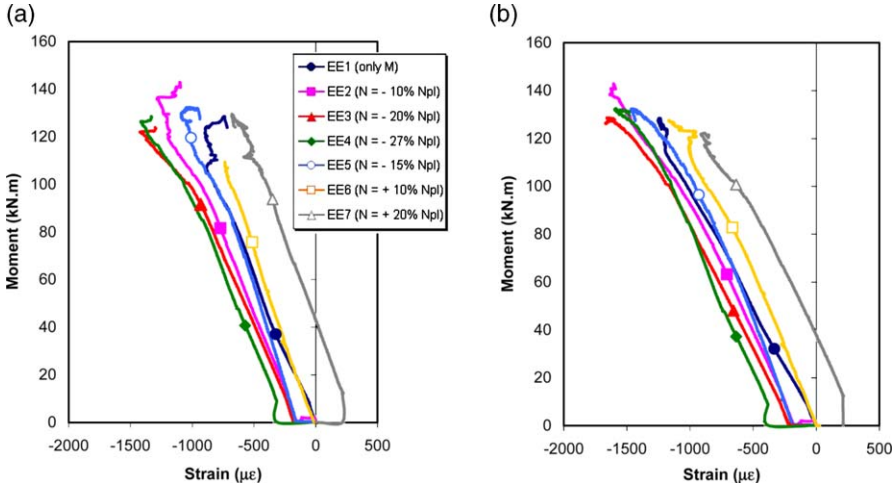


Fig. 14. Column web in compression (2)—moment versus strain curves. (a) Strain gauge number 11 and (b) channel 14 of rosette C.

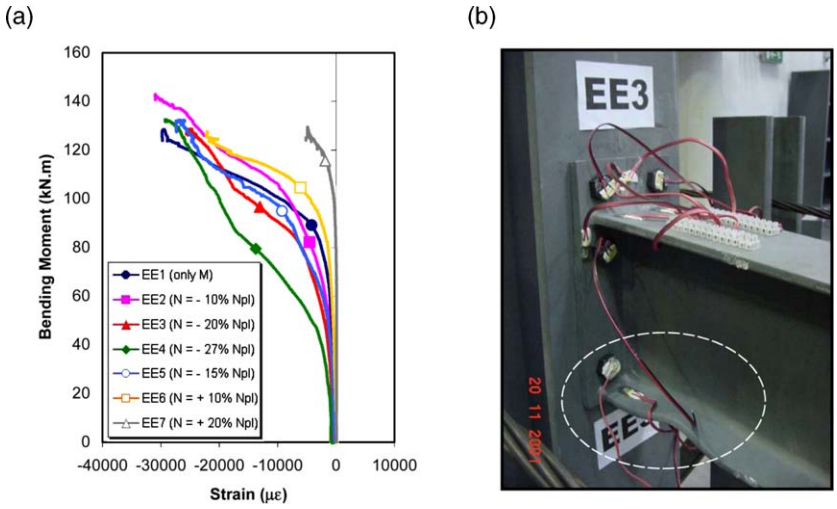


Fig. 15. Beam flange in compression (7)—moment versus strain curves. (a) Average of measured strains (strain gauges 29–32) and (b) beam flange and web in compression residual deformation.

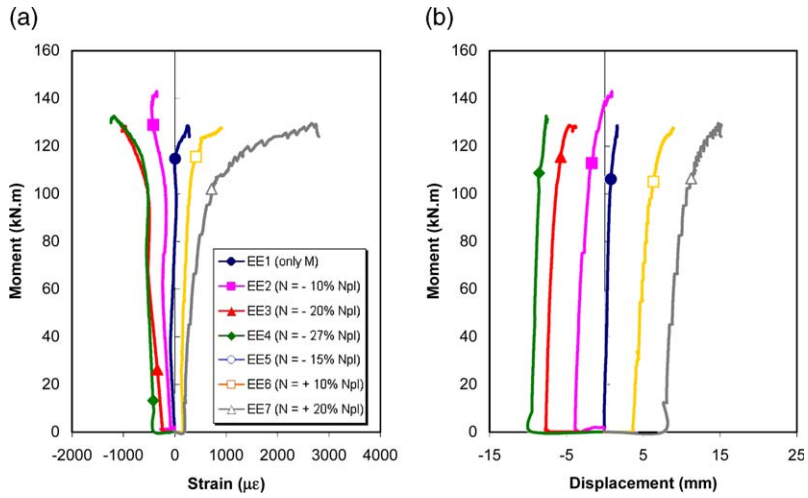


Fig. 16. Column flange in bending (4)—moment versus strain and moment versus displacement curves. (a) Strain gauge number 10 and (b) LVDT 7 measured displacements.

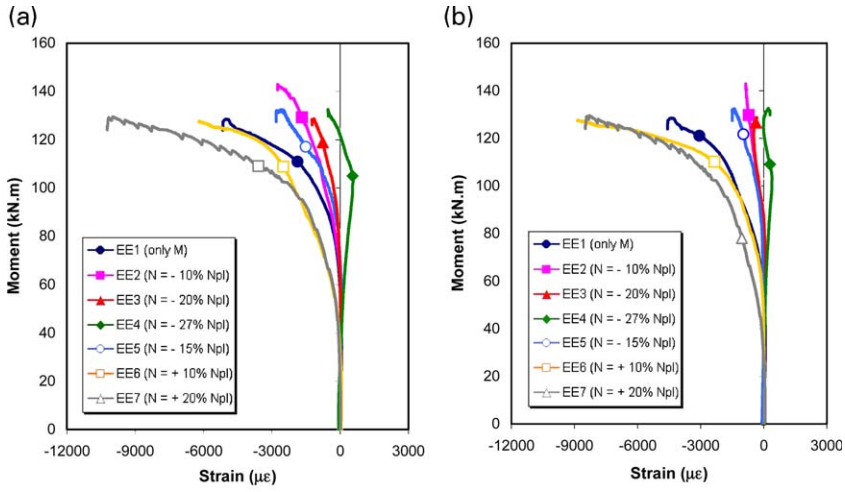


Fig. 17. Endplate in bending (5)—moment versus strain curves. (a) Strain gauge number 23 and (b) strain gauge number 24.

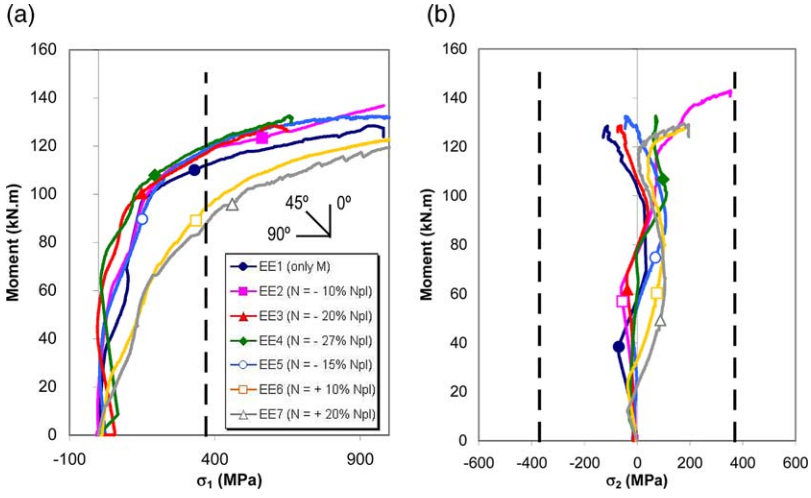


Fig. 18. Endplate in bending (5)—moment versus principal stresses curves. (a) Principal stresses—$\sigma_1$ and (b) principal stresses—$\sigma_2$.

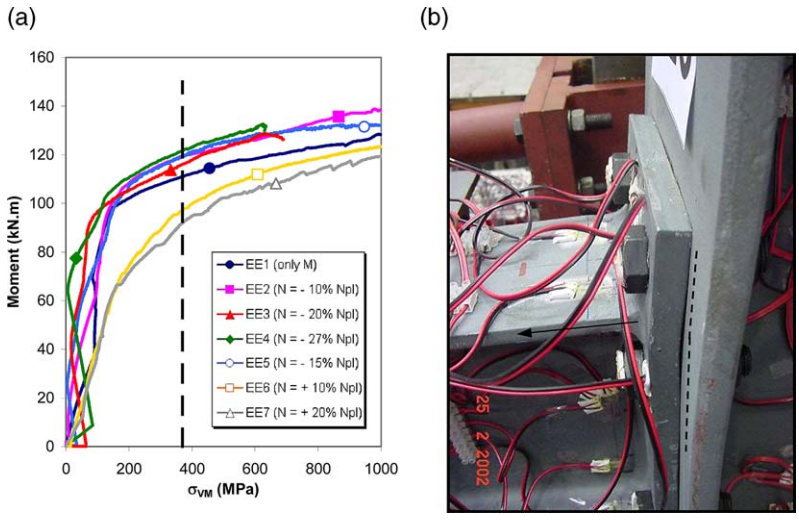


Fig. 19. Endplate in bending (5)—moment versus *von Mises* stresses curves. (a) *von Mises* stresses and (b) endplate in bending residual deformations.

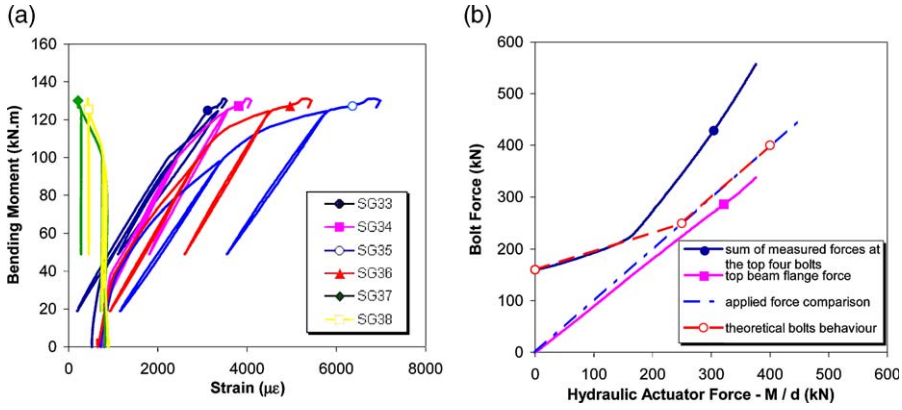


Fig. 20. Bolts in tension (10)—moment versus strain curves (EE1 test).

remained in compression, thus validating the hypothesis that this bolt row did not contribute to the joint bending resistance. In this test, prying forces were observed, Fig. 20(b). This figure shows a comparison between the hydraulic actuator applied force and the measured force in the top four bolts.

Fig. 21 depicts the moment versus strain results for one of the compressive axial force tests, EE4. In this

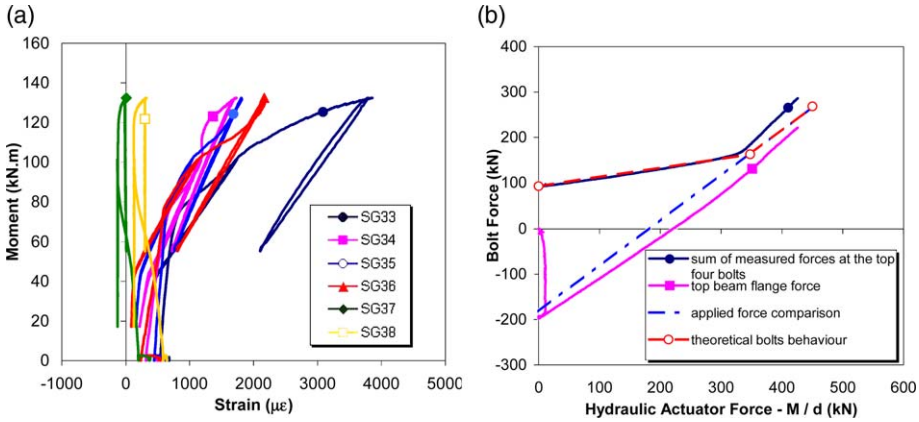


Fig. 21. Bolts in tension (10)—moment versus strain curves (EE4 test).

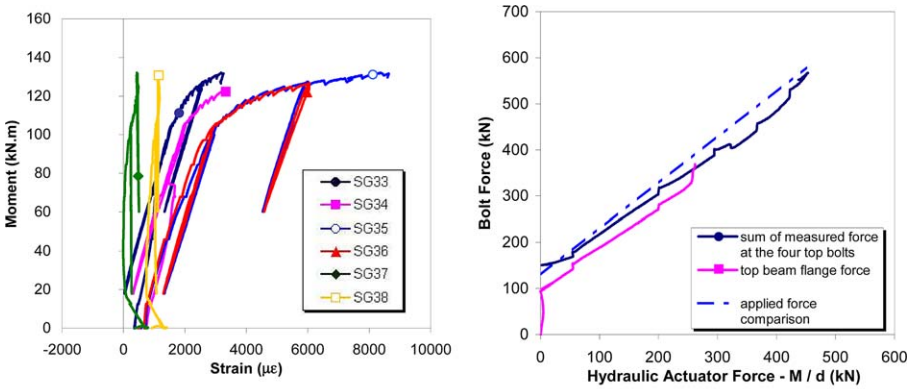


Fig. 22. Bolts in tension (10)—moment versus strain curves (EE7 test).

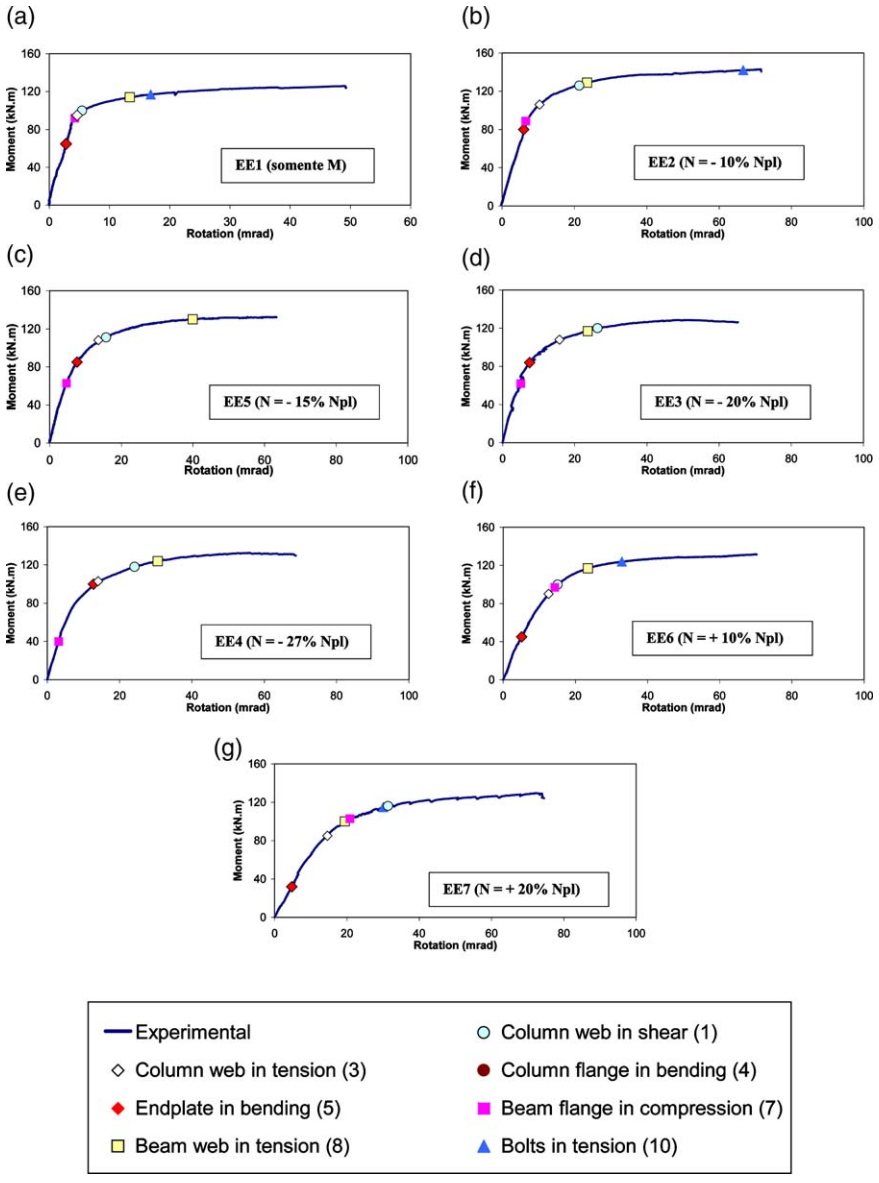


Fig. 23. Yielding sequence of the components.

case, the presence of the axial force decreases the bolt load maintaining the applied bottom bolt forces in compression.

Test EE7 did not exhibit prying forces because of premature separation between the endplate and the beam flange upon application of the tensile axial force. This is illustrated in Fig. 22.

Fig. 23 summarizes, for each test, the sequence of yielding for all components. It clearly shows that, as noted before, with increasing compressive force, the beam flange in compression becomes progressively more critical. Analogously, with increasing tension forces, the endplate in bending becomes the critical component.

### 3.4. Interaction diagrams

The results of Fig. 23 can be condensed in an *M–N* interaction diagram that illustrates the variation of yielding of each component, shown in Fig. 24.

Fig. 25 illustrates the *M–N* interaction diagram corresponding to: (i) the elastic resistance of the joint (taken as yielding of the first component); (ii) the plastic resistance, taken, either as (ii.1) the moment corresponding to a secant stiffness of $S_{j,ini}/2$, or (ii.2) a secant stiffness of $S_{j,ini}/3$ [21], and (iii) the maximum resistance. Unfortunately, collapse was never reached during the tests.

## 4. Conclusions

This paper presented an experimental programme on extended endplate beam-to-column joints under bending and axial force (tension/compression) carried out at the University of Coimbra, Portugal. The main conclusions of this investigation were:

(i) The moment–rotation curves for all tests indicate that the presence of the axial force significantly affects the joint structural behaviour. The maximum bending moment resistance was obtained

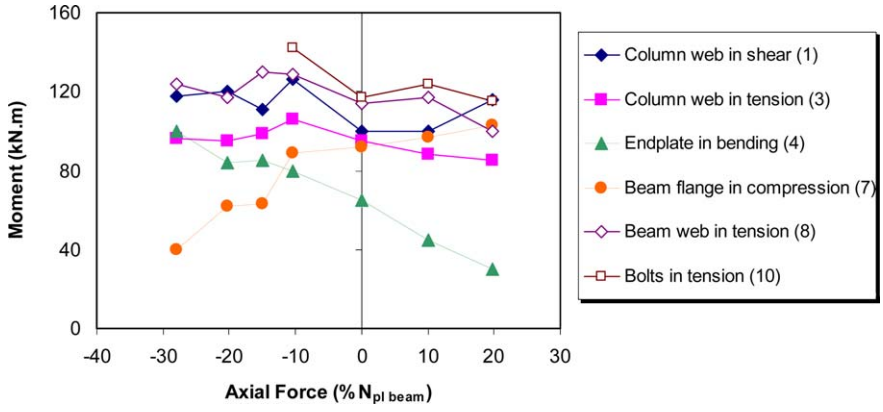


Fig. 24. *M–N* interaction diagram for each individual component.

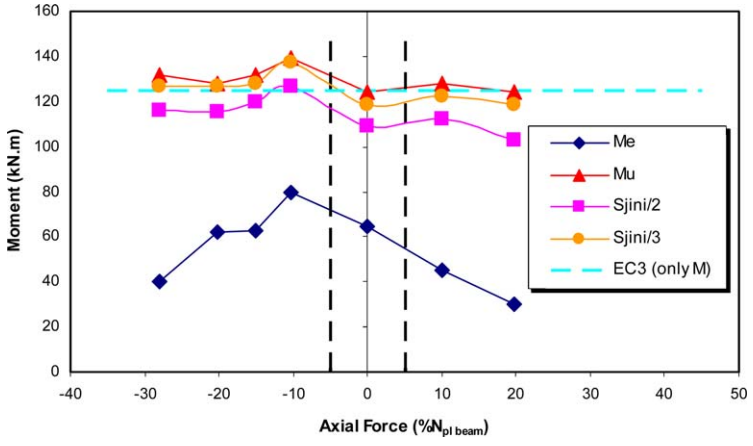


Fig. 25. *M–N* interaction diagram.

in test EE2 whose compressive axial force level corresponded to 10% of the beam plastic resistance, a value 6% greater than test EE1 (without any axial load). In contrast, in the two tests with tensile axial forces, EE6 and EE7, the bending moment resistance was less than test EE1 due to the premature mobilization of the joint tension zone components.

(ii) It was also verified that the compression zone critical component was the beam flange in compression while for the tension zone, the critical component was the endplate in bending, results already predicted using the specifications of part 1.8 of EC3.

The use of component models to estimate the moment versus rotation/axial force–displacement response of beam-to-column joints subjected to bending moment and axial force is not a straightforward extension of similar models (see Fig. 13) developed only for bending.

Firstly, depending on the loading history, the shift of neutral axis in the joint during loading is much more pronounced than in the pure bending case, requiring the assessment of the appropriate unloading behaviour of the joint components. Additionally, each component must present a distinct behaviour in tension and in compression. Both these aspects are illustrated in Fig. 26.

Secondly, the component model must consider all possible components, the concept of tension and compression zones being no longer applicable. A possible illustration of a component model for bending and axial force is shown in Fig. 27.

Finally, whenever multiple bolt rows are present, some additional phenomena such as stiffness coupling and group behaviour [21] are also crucial and can modify the response of the joint. These phenomena, recently extensively explored by Cerfontaine [21] probably explain the increase in bending resistance for low levels of axial compression.

To conclude, it is noted that before detailed analytical procedures for the response of beam-to-column joints under bending and axial force are proposed, detailed numerical simulations are still required, an issue being actively addressed by the authors.

## Acknowledgements

Financial support from "CAPES—Coordenação de Aperfeiçoamento de Pessoal de Nível Superior, Brazil" and "CNPq—Conselho Nacional de Desenvolvimento Científico e Tecnológico, Brazil" for the first author is gratefully acknowledged.

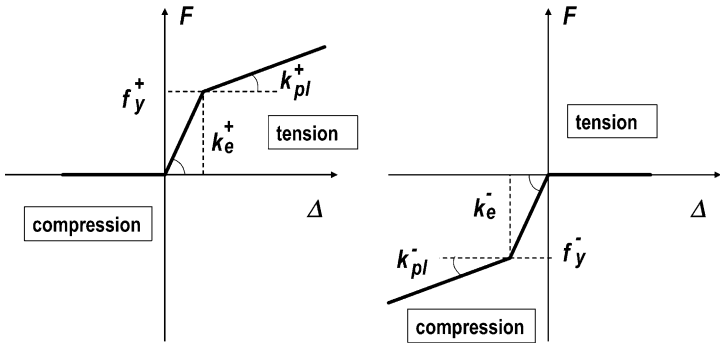


Fig. 26. Typical component behaviour.

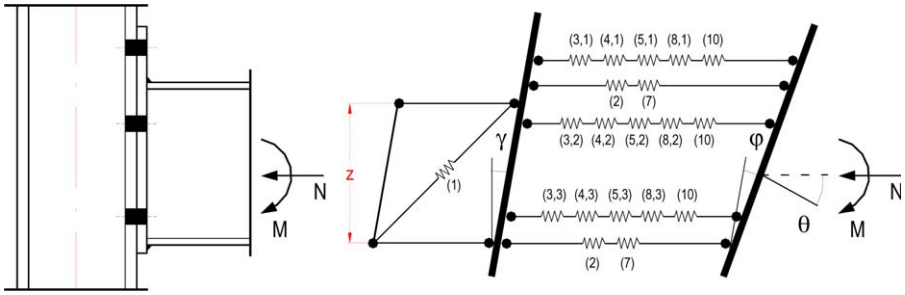


Fig. 27. Component model for *M–N* interaction.

## References


[1] Eurocode 3. prEN 1993-1-8: 2003, Part 1.8: design of joints, Eurocode 3: design of steel structures, Stage 49 draft., 5 May 2003. Brussels: CEN, European Committee for Standardisation; 2003.

[2] Eurocode 3. ENV—1993-1-1:1992/A2, Annex J, design of steel structures—joints in building frames. Document CEN/TC 250/SC 3. Brussels: CEN, European Committee for Standardisation; 1998.

[3] Wald F, Jaspart JP. Stiffness design of column bases. Journal of Constructional Steel Research 1998;46(1–3):245 [paper no. 135].

[4] Pertold J, Xiao RY, Wald F. Embedded steel column bases I. Experiments and numerical simulation. Journal of Constructional Steel Research 2000;56:253–70.

[5] Pertold J, Xiao RY, Wald F. Embedded steel column bases II. Design model proposal. Journal of Constructional Steel Research 2000;56:271–86.

[6] Guisse S, Vandegans D, Jaspart J-P. Application of the component method to column bases. Experimentation and development of a mechanical model for characterization. Rapport CRIF, MT 295. CRIF, Liège, 1997.

[7] Wald F, Švarc M. Experiments with end plate joints subject to moment and normal force. Contributions to experimental investigation of engineering materials and structures. CTU Reports No.: 2–3, Prague, 2001. p. 1–13.

[8] Simões da Silva L, Lima L, Vellasco P, Andrade S. Proceedings of the First International Conference on Steel and Composite Structures, Pusan, 2001. Experimental and numerical assessment of beam-to-column joints under bending and axial force, vol. 1. Seoul: Techno Press; 2001, p. 715–22.

[9] Simões da Silva L, Lima L, Vellasco P, Andrade S. Behaviour of flush end-plate beam-to-column joints under bending and axial force. Steel and Composite Structures 2004;4(2):77–94.

[10] Lima L. Behaviour of endplate beam-to-column joints under bending and axial force. Ph.D. Thesis. PUC-Rio, Pontifical Catholic University, Civil Engineering Department, Rio de Janeiro, Brazil, 2003 [in Portuguese].

[11] Jaspart J-P. Recent advances in the field of steel joints. Column bases and further configurations for beam-to-column joints and beam splices. Department MSM, University of Liège; 1997.

[12] Jaspart J-P. General report: session on connections. Journal of Constructional Steel Research 2000;55:69–89.

[13] Finet L. Influence de l'effort normal sur le calcul des assemblages semi-rigides. CUST, Clermont-Ferrand. Travail de Fin d'Etudes, CRIF, Liège, 1994 [in French].

[14] Cerfontaine F. Etude analytique de l'interaction entre moment de flexion et effort normal dans les assemblages boulonnés. Construction Métalique 2001;4:1–25 [in french].

[15] Silva LS, Coelho AG. An analytical evaluation of the response of steel joints under bending and axial force. Computers and Structures 2001;79:873–81.

[16] Cruz PJS, Simões da Silva L, Rodrigues DS, Simões RAD. Database for the semi-rigid behaviour of beam-to-column connections in seismic regions. Journal of Constructional Steel Research 1998;46(1–3):paper no. 120.

[17] Sokol Z, Wald F, Delabre V, Muzeau JP, Svarc M. Design of end plate joints subject to moment and normal force. Proceedings of the Third European Conference on Steel Structures—Eurosteel 2002, Coimbra 2002. Coimbra: Cmm Press; 2002, p. 1219–28.

[18] EN 10002. Metallic materials—tensile tests. Part 1: Method of test (at ambient temperature). Brussels: CEN, European Committee for Standardisation; 1990.

[19] EN 10020. Steel definition and classification. Brussels: CEN, European Committee for Standardisation; 1989.

[20] EN 10025. Hot rolled products of non-alloy structural steel. Brussels: CEN, European Committee for Standardisation; 1994.

[21] Cerfontaine F. Bending moment and axial force interaction in bolted joints. Ph.D. Thesis. University of Liège, 2003 [in French].